Self Ionization Probabilities Following De-excitation Decay of K-Shell Vacancy in Atoms $Z = 10$–80

Adel Mohammedein EL-SHEMI

Applied Sciences Department, College of Technological Studies,
P.O. Box 42325, Shuwaikh 70654, KUWAIT
e-mail: elshemi1999@hotmail.com

Abstract

The average number of ejected electrons and the probability of ion charge state distributions following K-shell ionization in atoms from $Z = 10$ to $Z = 80$ were calculated. Monte Carlo simulation technique was used to simulate all possible pathways of radiative and non-radiative transitions to fill the inner-shell ionization in excited atoms. The radiative and non-radiative branching ratios were calculated from Multiconfiguration Dirac-Fock (MCDF) and Dirac-Fock-Slater (DFS) wave functions. The average number of ejected electrons in atoms with $Z = 10$ is about two, because the non-radiative transitions exceed radiative transitions by 98%. The mean number of ejected electrons increases with atomic number Z. The results of ion charge state distributions and mean ejected number agree well with available experimental values.

Key Words: Atomic properties, Auger vacancy cascades, ion charge state distributions.

1. Introduction

The inner-shell electron of an atom can be ionized by a soft x-ray; the inner-shell vacancy then decays through either radiative or non-radiative transitions. In the case of radiative transitions, the vacancy is filled with an electron from one of the outer-shells with emission of a photon; and that vacancy is in turn filled by an electron from a shell higher up, the whole process resulting in the emission of characteristic x-rays. For non-radiative transitions, one electron from an outer shell fills up the inner-shell vacancy and another electron is ejected into the continuum, resulting in two vacancies. If these new vacancies are not in the outermost shells, these are filled by subsequent radiative and non-radiative transitions. These vacancy cascades produce multiply-charged ions.

Investigation of the vacancy cascades following the original inner-shell vacancy, and the yield of multiply-ionized atoms connected with the cascades, is of interest to various fields of research, such as solid state physics, plasma physics and astrophysics.

The charge state distributions of ions resulting from de-excitation decay on inner-shell vacancies were studied both experimentally and theoretically. The multiply-charged ions following vacancy cascades in rare gas atoms were measured [1-5]. The photoionization energies to create the initial inner-shell vacancy was obtained from x-ray tubes, and the produced ions were analyzed with a magnetic spectrometer. The charge state distribution of the ions as a function of photon energies were measured by sweeping the photon energy

across the ionization threshold [6–10]. The initial inner-shell vacancy, produced by synchrotron radiation, and the yield ions are analyzed using a time-of-flight mass spectrometer.

There are two major approaches to calculate the vacancy cascades and multiply charged ions following inner-shell vacancy production in atoms. The first method is based on straightforward construction of the de-excitation decay trees for radiative and non-radiative transitions [1, 11–14]. The second method is based on simulation of all possible radiative and non-radiative pathways to fill the inner-shell vacancies [15–18].

In the present work, the probabilities of the final charge state distribution of ions, and the average number of ejected electrons that result from vacancy cascade de-excitation after the initial K-shell vacancy, are calculated for atoms $Z = 10$–80. The Monte Carlo (MC) method is applied to simulate all possible pathways of radiative and non-radiative transitions to fill the K-shell vacancy. The radiative (fluorescence) and non-radiative (Auger and Coster-Kronig) branching ratios are calculated using Multiconfiguration Dirac-Fock wave function and Dirac-Fock-Slater wave functions, respectively. The results of final charge state distributions and average number of electrons are compared with the available theoretical and experimental data.

2.   Method of Calculation

The calculation of final charge state distributions and average number of ejected electrons following de-excitation decay of inner-shell vacancies has been carried out using the Monte Carlo method. This method is based on the simulation of all possible radiative, non-radiative transitions and electron shake-off processes that lead to the filling of the inner-shell vacancies. For each vacancy, the program examines whether the electron shake-off process is possible or not using the total shake-off transition probabilities for the shells considered. When an electron shake-off process takes place, one electron is ejected from the atom's subshells and the number of vacancies is increased by one. The detailed description of the Monte-Carlo method has been given in previous papers [17, 18].

The radiative, non-radiative transitions and electron shake off processes are the principle mechanisms of a cascade originating from an inner-shell vacancy. The electron shake-off process is caused by the change of atomic potential, due to the creation of an inner-shell vacancy and the subsequent decay through radiative and non-radiative transitions. The radiative branching ratios (fluorescence yields) and non-radiative branching ratios (Auger yields) give valuable information on the de-excitation dynamic of an atom with an inner-shell vacancy, and are thus calculated. The radiative branching ratio ω is defined as the probability that a vacancy in an initial state i is filled and accompanied by radiative transitions in the form of characteristic emission of x-rays from state f, and is given by

$$\omega = \frac{A(if)}{A(i) + A(a)},\qquad(1)$$

where $A(if)$ is the radiative transition rate from initial state i to final state f, $A(i)$ is the total radiative decay rate of state i, and $A(a) = \sum_f A(a_{if})$ is the total Auger and Coster-Kronig decay rate of state f. The non-radiative branching ratios a are defined as the probability that the vacancy in an initial state i is filled through radiative transitions under emission of electrons state f, and is given by:

$$a = \frac{A(a_{if})}{A(i) + A(a)}.\qquad(2)$$

The radiative transition rates $A(if)$ for singly ionized atoms are calculated using Multiconfiguration Dirac-Fock (MCDF) wave functions from Grant et al. [19]. The non-radiative transition rates $A(a_{if})$ for single ionized atoms are calculated using the Dirac-Fock-Slater wave functions.

Analysis of each cascade start with consideration of all possible radiative and non-radiative transition rates with which the initial inner-shell vacancy in the atom can be filled. In the first step, one transition is chosen to fill the primary vacancy. If the decay occurs through radiative transition, the primary vacancy moves into an outer shell together with the emission of a characteristic x-ray. If the decay occurs through a non-radiative transition, the inner-shell vacancy jumps to a higher sub-shell and is accompanied by the emission of an (Auger) electron, causing the number of vacancies to increase by one. The choice of decay is random, the probabilities being proportional to the radiative and non-radiative branching ratios. After decay of the primary vacancy, new vacancies appear in the higher sub-shell. The decay of these vacancies occur through further radiative and or non-radiative transitions, randomly with the same considerations as in the first step, repeatedly occurring until the vacancies reach the outer-most shell. The number of vacancies in the outer-shells is recorded. After finishing with the vacancy cascade, the same initial inner-shell vacancy is again created and the cascade is again started and cycled. The probabilities of the final charge state distributions and the average number of ejected electron are found after 10^5 cascade simulations.

The principle mechanisms in these simulations are the radiative (x-rays), non-radiative (Auger and Coster-Kronig) transitions and electron shake-off process. The change of atomic potential that occurs due to the production of inner-shell vacancies in an atom and the subsequent de-excitation decays through radiative and non-radiative transitions, leads to the emission of additional electrons emitted to the continuum (the electron shake-off processes). The emission of photons and electrons, which accompany radiative and non-radiative transitions, is due to shifts of the binding energy levels. These shifts lead to significant changes in the radiative and non-radiative transition rates of atoms with multiple vacancies. These changes of radiative and non-radiative transition rates as result of multiple vacancy formation have been calculated using a statistical weighting procedure [20].

The consideration of the electron-shake off processes and the changes of radiative and non-radiative transition rates as result of multiple vacancy formation play an important rule in the calculations of the final charge state distributions and in the mean number of ejected electrons.

3. Results and Discussion

The radiative (fluorescence) yield and non-radiative (Auger) yield for K-shell ionization are presented as a function of atomic number Z in Figure 1. The radiative branching ratios were calculated from equation (1) and the non-radiative branching ratios from equation (2). The fluorescence yield increase smoothly and Auger yields decrease with increasing the atomic number Z. For low Z atoms, the non-radiative yields are higher than the radiative yields, and the radiative yields are higher than non-radiative in high Z atoms.

Figure 2 shows the probability of ejection electrons $p(i)$ following de-excitation vacancy cascades after the initial K-shell vacancy in atoms up to $Z = 80$. The probability of doubly charged ions $p(2)$ is high in light atoms up to neon ($10 \leq Z$). There are four possible paths available for filling a K-vacancy in light atoms up to $10 \leq Z$. For the first path, the initial K-vacancy transfers into L-subshells, accompanied by the emission of a characteristic x-ray. According to radiative and non-radiative branching ratios, the filling of K-vacancies in light atoms occur by Auger transitions more probable than by radiative transitions. As shown in Figure 1, for K-vacancies in neon, the fluorescence yield to Auger yield ratio is 0.7% :93.3% ; the decay of K-shell vacancies occurs with higher probability under Auger transitions than under radiative transitions. The other three decay paths occur through non-radiative transitions with 93% total probability. The decay of K-vacancy involves pairs of electrons as follows: (L_{23}, L_{23}), (L_1, L_{23}) and (L_1, L_1). If the vacancy is created in the L subshell, no radiative and non-radiative Auger processes can occur. Then the filling of L-subshell vacancies in light atoms up to Ne is not possible through radiative and non-radiative transitions. The reason is related to the selection rules for dipole transitions, and that the probability for a radiative transitions being negligible, and that the Auger processes are not permitted. Then the filling of K-vacancy through Auger transitions result in $p(2)$ ions and the atoms remain doubly charged. Beginning with sodium

($Z = 11$), aside from KLL Auger transitions, other radiative and non-radiative transitions appear during the de-excitation cascades. In these transitions from the filling of the original K-shell vacancy, the atoms emerge with ionization degree above two. As shown in Figure 2, the probability $p(4)$ increased while $p(2)$ rapidly decreased. The creation of L-subshell vacancies in atoms above neon may be filled through LLM and LLN Coster-Kronig transitions. This means that the probability of charged ions, $p(4)$, is more significant than the probability of charged ions $P(2)$. On the contrary, for heavy atoms Z = 40–80, the probability of charged ions, $P(4)$, is low, as shown in Figure 2., because the number of ejected electrons increase with increasing the atomic structure. The probability $p(6)$ of emitting six electrons following the initial K-vacancy production is highest for $18 \leq Z \leq 80$. Iron ($Z = 26$) is found to have the highest probability for ejecting 8 electrons. For high-Z, the contributions of Auger and Coster-Kronig processes lead to production of $p(10)$ and $p(12)$ charged ions. For K-shell de-excitation, an increasing broadening of the resulting ion charge state distribution appears due to the increasing complex atomic structure and the de-excitation channels connected with it.
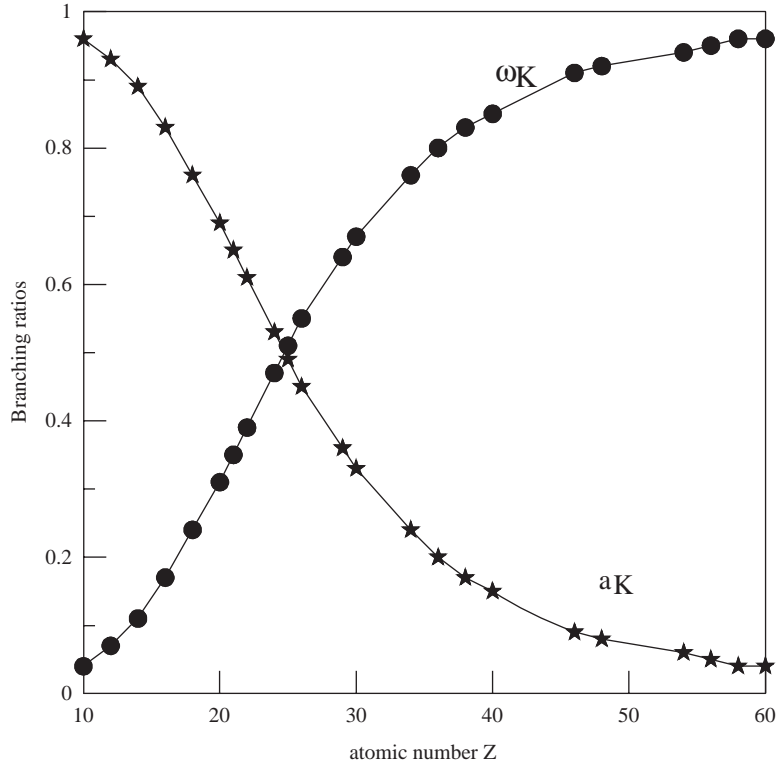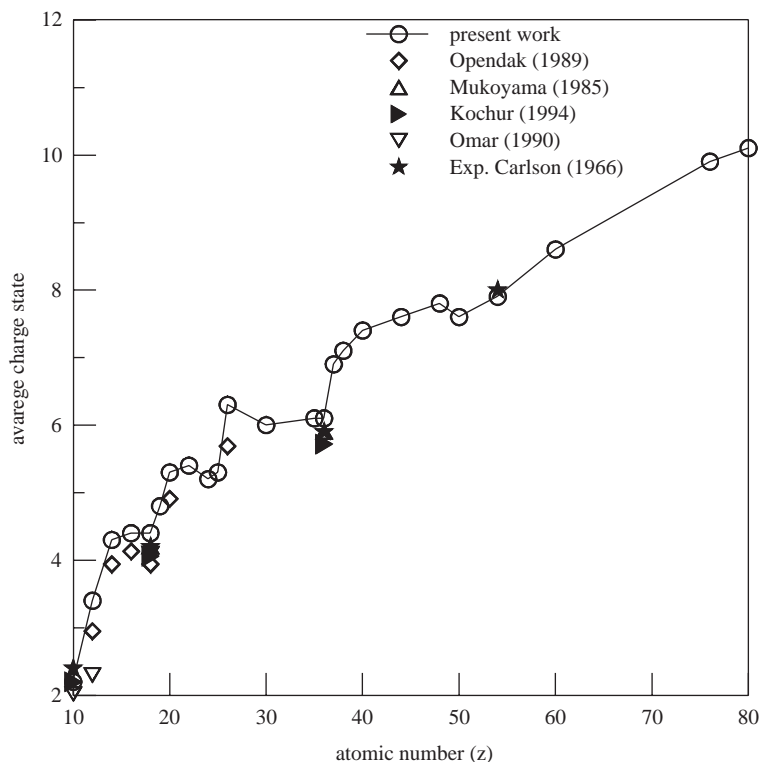

Figure 1. The radiative branching ratios (ω_K) and non-radiative branching ratios (a_K) as function of atomic number Z.

The average number of ejected electrons that result from de-excitation cascades after initial K-shell vacancy production, for atoms up to $Z = 80$, are given in Figure 3. In atoms with $Z \leq 10$, Auger transition energies are not allowed after reaching vacancies in L outer-shells. However, the average number of ejected electrons that results after K-shell ionization in these atoms is about two electrons. The average number of ejected electrons increases with $Z > 10$ due to additional allowed Auger and Coster-Kronig channels. In the case of $11 \leq Z \leq 37$, abrupt changes are found in the average charge. The alkali atoms ($Z = 11, 19, 37$) have an additional luminous electron to the configuration of the rare gases atoms. This luminous electron is weakly bound and has small ionization energy. Therefore beginning with these elements, the average number of ejected electrons result from de-excitation cascades after K-shell vacancy production rapidly increases with Z; and at the same time, the vacancy cascades become more complex when one goes to heavier atoms (at

least when the initial hole is created in the K-shell). The results presented in the Figures 2 and 3 give a complete and detailed picture about the Z-dependence of the probabilities of the charge state distributions $p(i)$ and the mean ejected number of electrons after K-shell ionization in atoms up to $Z = 80$.
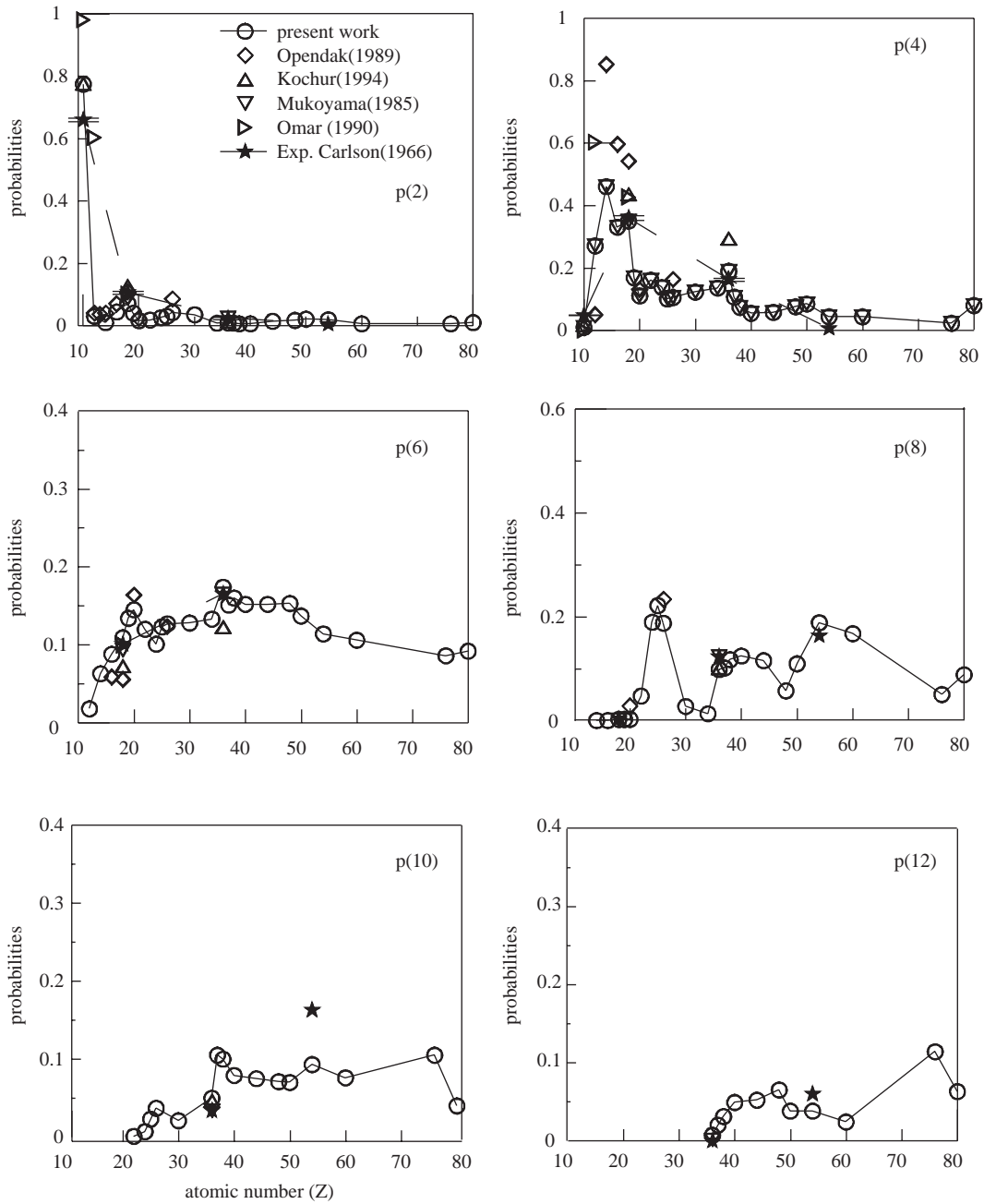
Figure 2. The probabilities of charge state distributions following K-shell vacancy production as function of atomic number Z.

Figure 3. The average number of ejected electrons following K-shell vacancy as function of atomic number Z.

4.   Conclusion

The ion charge state distributions and average ion charges following cascading de-excitation of atomic K-shell vacancies in atoms $Z = 10$–80 were calculated. The simulation technique generates trees of all possible pathways for radiative and non-radiative transitions to fill the inner-shell vacancies. The calculations of the de-excitation cascades are based on the radiative and non-radiative branching ratios in the course of cascade development. The radiative and non-radiative transition rates were calculated using MCDF wave functions and DFS wave functions. For K-shell de-excitation decays, an increasing broadening of the resulting ion charge state distributions and average number of ejected electrons appear with increasing Z and the de-excitation Auger and Coster-Kronig channels, which connected with Z. The ion charge state distributions and mean charged ions are compared with the available theoretical and experimental data. The results agree well with the experimental values. Calculation results show a permanent increase in the number of ejected electrons with increasing complexity of the atomic structure. The vacancy following inner-shell ionization is one possible method for production of highly charged ions without high momentum transfer. This method is an interesting alternative instead of using high energetic collision processes.

References

[1] M. O. Krause, M. V. Vestal, W. H. Johnson, T. A. Carlson; *Phys. Rev.*, **133**, (1964), 385–90.

[2] T.A. Carlson and M.O. Krause; *Phys. Rev.*, **A137**, (1965), 1655.

[3] T.A. Carlson and M.O. Krause; *Phys. Rev. Letters,* **14**, (1965), 390.

[4] T.A. Carlson, W.E. Hunt, and M.O. Krause; *Phys. Rev.*, **A151**, (1966), 41–47.

[5] T.A. Carlson and M.O. Krause; *Phys. Rev.*, **A140**, (1965), 1054.

[6] K. Ueda, E. Shigemasa, T. Sato, A. Yagishita, M. Ukai, H. Maezawa, T. Hayaishi and T. Sasaki; *J. Phys. B: At. Mol. Opt. Phys.*, **24**, (1991), 605.

[7] T. Hayaishi, Y. Morioka, Y. Kageyama, M. Watanabe, I.H. Suzuki, A. Mikuni, G. Isoyama, S. Asaoka and M. Nakamura; *J. Phys. B: At. Mol. Phys.*, **20**, (1987), L287.

[8] T. Mukoyama, T. Tonuma, A. Yagishita, H. Shibata, T. Matsuo, K. Shima and H. Tawara; *J. Phys. B: At. Mol. Phys.*, **20**, (1987), 4453.

[9] N. Saito and I.H. Suzuki; *J. Phys. B: At. Mol. Opt. Phys.*, **25**, (1992), 1785.

[10] H. Tawara, T. Hayaishi, T. Koizumi, T. Matsuo, K. Shima and A. Yagishita; *J. Phys. B: At. Mol. Opt. Phys.*, **25**, (1992), 1476.

[11] G. Omar and Y. Hahn; *Phys. Rev. A,* **43**, (1991), 4695.

[12] G. Omar and Y. Hahn; *Phys. Rev. A,* **44**, (1991), 483.

[13] A.G. Kochur, A.I. Dudenko, V.L. Sukhorukov and I.D. Petrov; *J. Phys. B: At. Mol. Opt.,* **27**, (1994), 1709.

[14] A.G. Kochur, A.I. Dudenko, V.L. Sukhorukov and I.D. Petrov; *J. Phys. B: At. Mol. Opt.,* **28**, (1995), 387.

[15] T. Mukoyama; *Bull. Inst. Chem. Res. Kyoto Univ.*, **63**, (1985), 373.

[16] N. Mirakhmedov and E. S. Parilis; *J. Phys. B: At. Mol. Opt. Phys.*, **21**, (1988), 795.

[17] A.M. El-Shemi, A.A. Ghoneim and Y.A. Lotfy; *Turk. J. Phys.*, **27**, (2003), 51.

[18] A.H. Abdullah, A.M. El-Shemi and A.A. Ghoneim; *Rad. Phys. and Chem.*, **68**, (2003), 697.

[19] I.P. Grant, B.J. Mckenzie, P. Norrington, D.F. Mayers and N.C. Pyper; *Comput. Phys. Commun.*, **21**, (1980), 207.

[20] V.L. Jacobs, J. Davis, F.B.F. Rozsnyai and J.W. Cooper; *Phys. Rev. A*, **21**, (1980), 1917.